


θ -dependence and center symmetry in Yang-Mills theories

Claudio Bonati^{✉,*}, Marco Cardinali^{✉,†}, Massimo D'Elia[‡], and Fabrizio Mazziotti^{✉,§}

*Dipartimento di Fisica dell'Università di Pisa and INFN—Sezione di Pisa,
Largo Pontecorvo 3, I-56127 Pisa, Italy*

 (Received 20 December 2019; accepted 27 January 2020; published 11 February 2020)

We investigate the relation between the realization of center symmetry and the dependence on the topological parameter θ in $SU(N)$ Yang-Mills theories, exploiting trace deformations as a tool to regulate center symmetry breaking in a theory with a small compactified direction. We consider, in particular, $SU(4)$ gauge theory, which admits two possible independent deformations, and study, as a first step, its phase diagram in the deformation plane for two values of the inverse compactified radius going up to $L^{-1} \sim 500$ MeV, comparing the predictions of the effective one-loop potential of the Polyakov loop with lattice results. The θ -dependence of the various phases is then addressed, up to the fourth order in θ , by numerical simulations; results are found to coincide, within statistical errors, with those of the standard confined phase iff center symmetry is completely restored and independently of the particular way this happens, i.e., either by local suppression of the Polyakov loop traces or by long range disorder.

DOI: [10.1103/PhysRevD.101.034508](https://doi.org/10.1103/PhysRevD.101.034508)

I. INTRODUCTION

Pure gauge theories, defined on a space-time with one or more compactified directions, possess a symmetry under global transformations, which can be classified as gauge transformations respecting the periodicity but for a global element of the center of the gauge group [e.g., \mathbb{Z}_N for $SU(N)$ gauge theories]; this is known as center symmetry. Such symmetry regulates most of the phase structure of the pure gauge theory, undergoing spontaneous symmetry breaking for small enough compactification radii, and the Polyakov loop (holonomy) around the compactified direction is a proper order parameter for its realization. When the compactified direction is the thermal Euclidean direction, the transition is associated to deconfinement, and the Polyakov loop is defined as

$$P(\vec{x}) = \mathcal{P} \exp \left(i \int_0^L A_0(\vec{x}, \tau) d\tau \right); \quad (1)$$

its trace vanishes in the confined phase ($\langle \text{Tr} P \rangle = 0$), while it is different from zero for $T > T_c$, where T_c is

the deconfinement critical temperature [e.g., for $SU(N)$, $\langle \text{Tr} P \rangle = \alpha e^{i2\pi n/N}$, with $n \in \{0, 1, \dots, N-1\}$ and $\alpha > 0$].

Yang-Mills theories are characterized by many other nonperturbative properties, the relation to center symmetry of which is still not clear. Among them, a significant role is played by the dependence on the topological parameter θ , which enters the (Euclidean) Lagrangian as follows,

$$\mathcal{L}_\theta = \frac{1}{4} F_{\mu\nu}^a(x) F_{\mu\nu}^a(x) - i\theta q(x), \quad (2)$$

where $q(x)$ is the topological charge defined by

$$q(x) = \frac{g^2}{64\pi^2} \epsilon_{\mu\nu\rho\sigma} F_{\mu\nu}^a(x) F_{\rho\sigma}^a(x). \quad (3)$$

A nonzero θ breaks CP symmetry explicitly, and a nontrivial dependence on it is induced by gauge configurations with nontrivial winding number $Q = \int d^4x q(x)$ populating the path integral of the theory. The relevant information is contained in the free energy density $f(\theta)$, which around $\theta = 0$ can be usefully parametrized as a Taylor expansion as follows [1],

$$f(\theta) = f(0) + \frac{1}{2} \chi \theta^2 (1 + b_2 \theta^2 + b_4 \theta^4 + \dots), \quad (4)$$

where the topological susceptibility χ and the coefficients b_{2n} can be related to the cumulants of the topological charge distribution at $\theta = 0$ by the relations

$$\chi = \frac{\langle Q^2 \rangle_{c,\theta=0}}{\mathcal{V}}, \quad b_{2n} = (-1)^n \frac{2 \langle Q^{2n+2} \rangle_{c,\theta=0}}{(2n+2)! \langle Q^2 \rangle_{c,\theta=0}}, \quad (5)$$

where \mathcal{V} is the four-dimensional volume.

* claudio.bonati@unipi.it
† marco.cardinali@pi.infn.it
‡ massimo.delia@unipi.it
§ fabrizio.mazziotti@pi.infn.it

Published by the American Physical Society under the terms of the Creative Commons Attribution 4.0 International license. Further distribution of this work must maintain attribution to the author(s) and the published article's title, journal citation, and DOI. Funded by SCOAP³.

General large- N arguments [2–4] predict that, in the low temperature confined phase of the theory, the susceptibility stays finite in the large- N limit, while the b_{2n} are suppressed by increasing powers of $1/N$, as follows:

$$\chi = \chi_\infty + O(N^{-2}), \quad b_{2j} = O(N^{-2j}). \quad (6)$$

Such predictions have been checked successfully both for χ [5–8], with χ_∞ turning out to be compatible with the value predicted by the Witten-Veneziano solution to the $U_A(1)$ problem [9,10], and for the fourth order coefficient b_2 [6,11–16].

On the other hand, at asymptotically large T , i.e., small compactification radius, the theory becomes weakly coupled, and one expects that instanton calculus can be safely applied, leading to the validity of the dilute instanton gas approximation (DIGA) [17,18]

$$f(\theta) - f(0) \simeq \chi(T)(1 - \cos \theta) \\ \chi(T) \simeq T^4 \exp[-8\pi^2/g^2(T)] \sim T^{-\frac{11}{3}N+4}, \quad (7)$$

which predicts that the topological susceptibility vanishes exponentially fast with N , while the b_{2n} coefficients stay constant (for instance $b_2 = -1/12$), contrary to the large- N low- T scaling. The asymptotically large temperature at which DIGA should set in is not known *a priori*; moreover, while the prediction for $\chi(T)$ comes from a one-loop computation, the $(1 - \cos \theta)$ dependence expresses the fact that instantons and anti-instantons can be treated as independent, noninteracting objects, which is the essential feature of DIGA, and this could be true far before perturbative estimates become reliable.

In fact, various theoretical arguments [19–21] support the idea that the change of regime should take place right after T_c , and faster and faster as N increases. This scenario is strongly supported by lattice computations; the topological susceptibility drops at T_c [7,22–26], and it does so faster and faster as N increases, pointing to a vanishing of χ right after T_c in the large- N limit [7,24]. The vanishing of χ might not be enough to prove that DIGA sets in,¹ so that a stronger and definite evidence comes from studies of the coefficient b_2 , proving that it reaches its DIGA value right after T_c , and faster and faster as N increases [26,33].

As a consequence of the drastic change in the θ -dependent part of the free energy around T_c , the critical temperature itself is affected by the introduction of a nonzero θ ; in particular, T_c turns out to be a decreasing function of θ [34–36].

¹There are various examples of quantum field theories with nontrivial θ -dependence where χ is predicted to vanish in some limit, while the b_{2n} coefficients do not reach their DIGA values, like CP^{N-1} models in two dimensions and in the large- N limit [16,27–29] or QCD with dynamical fermions in the chiral limit [30–32].

The facts summarized above point to a strict relation between the realization of center symmetry and the θ -dependence of $SU(N)$ Yang-Mills theories, which one would like to investigate more closely. A powerful tool, in this respect, is represented by trace deformed Yang-Mills theories, which have been introduced in Ref. [37], although already explored by lattice simulations in Ref. [38]. The idea, which is inspired by the perturbative form of the Polyakov loop effective action at high temperature [17], is to introduce one or more (depending on the gauge group) center-symmetric couplings to the Polyakov loop and its powers, so as to inhibit the spontaneous breaking of center symmetry even in the presence of an arbitrarily small compactification radius. In this way, one can approach the weak coupling regime, where semiclassical approaches are available, while keeping center symmetry intact, so that the relation with θ -dependence can be investigated more systematically.²

Several works have already considered the use of trace deformed theories and also possible alternatives, like the introduction of adjoint fermions or the use of nonthermal boundary conditions [39–59]. There are actually already well definite semiclassical predictions regarding θ -dependence in the center-symmetric phase [37,60–62], which come essentially from the fact that in the limit of small compactification radius the deformed theory can be described in terms of noninteracting objects with topological charge $1/N$ [a sort of dilute fractional instanton gas approximation (DFIGA)]. This leads one to predict $f(\theta) - f(0) \propto 1 - \cos(\theta/N)$, hence for instance $b_2 = -1/(12N^2)$. While these predictions are in agreement with general large- N scaling for the confined phase exposed above, they are not in quantitative agreement with the lattice results for the confined phase, which yield instead $b_2 = -0.23(3)/N^2$ [16]; in addition, also the topological susceptibility itself is predicted to show significant deviations, for large N and small compactification radius [60], from the behavior shown in the standard confined phase.

It is therefore quite remarkable that, instead, lattice results obtained for $SU(3)$, which have been reported for the first time in Ref. [63], show that one recovers exactly the same θ -dependence as in the confined phase (i.e., the same value, within errors, for both χ and b_2) as soon as the trace deformation is strong enough to inhibit the breaking of center symmetry. The disagreement with semiclassical predictions is not a surprise, since the values of the compactification radius L explored in Ref. [63] go up to $L^{-1} \equiv T \approx 500$ MeV, while the condition for the validity of the semiclassical approximation is $T \gg N\Lambda$ where Λ is the nonperturbative scale of the theory, so that $T \sim 500$ MeV is

²Of course, this offers the possibility of investigating the connection of center symmetry to many other nonperturbative features of Yang-Mills theory, although in the present study, we are exclusively concerned with θ -dependence.

a scale where nonperturbative corrections can still be important. What is a surprise, claiming for further investigations, is the fact that such nonperturbative corrections are exactly the same as in the standard confined phase, leading to the same θ -dependence also from a quantitative point of view.

The purpose of the present study is to make progress along this line of investigation, by extending the results of Ref. [63] to larger $SU(N)$ gauge groups, considering in particular the case $N = 4$. There are various reasons to expect that the study of $SU(4)$ may lead to new nontrivial insights. Apart from the fact that the space of trace deformations extends to two independent couplings, we have that the possible breaking patterns of the center symmetry group \mathbb{Z}_4 are more complex, including also a partial $\mathbb{Z}_4 \rightarrow \mathbb{Z}_2$ breaking which corresponds to a phase differing from both the standard confined and the deconfined phase of the undeformed theory.

The way one can move across the different phases by tuning the two deformation couplings can be predicted based on the one-loop Polyakov loop effective potential. However, as we will discuss, numerical simulations show the presence of nontrivial corrections induced by fluctuations, which lead to complete center symmetry restoration also when this is not expected. Moreover, one has the possibility of checking whether the θ -dependence of the standard confined phase is achieved just for complete or also after partial restoration of center symmetry.

The paper is organized as follows. In Sec. II, we review the definition of $SU(N)$ pure gauge theories in the presence of trace deformations, our lattice implementations, and the numerical strategies adopted to investigate θ -dependence. In Sec. III, we first compare the predictions of one-loop computations of the phase diagram with numerical results, then discuss the θ -dependence observed for the various phases. Finally, in Sec. IV, we draw our conclusions.

II. TECHNICAL AND NUMERICAL SETUP

To investigate the relation between center symmetry and θ -dependence, we will use, as already anticipated in Sec. I, trace deformed Yang-Mills theories. In order to inhibit the spontaneous breaking of center symmetry when the theory is defined on a manifold with a compactified dimension, new terms (the trace deformations) are added to the standard Yang-Mills action, which are directly related to traces of powers of Polyakov loops along the compactified direction.

The action of the trace deformed $SU(N)$ Yang-Mills theory is thus [37]

$$S^{\text{def}} = S_{\text{YM}} + \sum_{\vec{n}} \sum_{j=1}^{\lfloor N/2 \rfloor} h_j |\text{Tr} P^j(\vec{n})|^2, \quad (8)$$

where \vec{n} denotes a generic point on a surface orthogonal to the compactified direction, the h_j s are new coupling

constants, $P(\vec{n})$ is the Polyakov loop associated to the compactified direction, and $\lfloor \cdot \rfloor$ denotes the floor function. The number of possible trace deformations is equal to the number of independent, center-symmetric functions of the Polyakov loop; in general, for $N > 3$, more than one deformation could be needed, in order to prevent the possibility of a partial breaking of the center symmetry, with a nontrivial subgroup of \mathbb{Z}_N left unbroken.

In order to clarify this point, let us specialize to the case $N = 4$, which is the one that will be thoroughly investigated in the following, and it is the simplest case in which a partial breaking of center symmetry can take place. For $N = 4$, the action in Eq. (8) reduces to

$$S^{\text{def}} = S_{\text{YM}} + h_1 \sum_{\vec{n}} |\text{Tr} P(\vec{n})|^2 + h_2 \sum_{\vec{n}} |\text{Tr} P^2(\vec{n})|^2, \quad (9)$$

and complete restoration of \mathbb{Z}_4 requires the vanishing of the expectation values of the two traces, $\text{Tr} P$ and $\text{Tr} P^2$. *A priori*, none of the two new terms in the action is sufficient to guarantee complete center symmetry restoration: for instance, $M = \text{diag}(1, 1, -1, -1)$ has $\text{Tr} M = 0$ but $\text{Tr} M^2 \neq 0$, while $M = \text{diag}(1, 1, i, -i)$ has $\text{Tr} M^2 = 0$ but $\text{Tr} M \neq 0$. If $\langle \text{Tr} P \rangle = 0$ and $\langle \text{Tr} P^2 \rangle \neq 0$ (a possibility which is forbidden if $N \leq 3$), center symmetry is spontaneously broken with the breaking pattern $\mathbb{Z}_4 \rightarrow \mathbb{Z}_2$, which corresponds to the fact that single quarks are confined but couples of quarks are not.

It thus seems that the term $|\text{Tr} P(\vec{n})|^2$ in the action is needed to force $\langle \text{Tr} P \rangle = 0$ and the term $|\text{Tr} P^2(\vec{n})|^2$ is needed to force $\langle \text{Tr} P^2 \rangle = 0$, but one should also take into account the following fact. Trace deformations are spatially local quantities; i.e., they tend to suppress $\text{Tr} P(\vec{n})$ and $\text{Tr} P^2(\vec{n})$ pointwise. However, the restoration of a global symmetry can also be induced by disorder, since order parameters are spatially averaged quantities, and this is what actually happens in many well-known cases, just like ordinary Yang-Mills theory (see, e.g., the discussion on the adjoint Polyakov loop in Ref. [63]). This will be particularly important in the following, when we present an analysis of the predicted phase diagram of the deformed $SU(4)$ gauge theory based on the one-loop effective potential of the Polyakov loop; this kind of analysis assumes a spatially uniform Polyakov loop, hence neglects the possibility of long-distance disorder. This is a possible explanation of the fact that numerical results will show sometimes deviations from the one-loop effective potential prediction, so that, for instance, center symmetry can be restored completely in some cases by adding just one trace.

The discretization of the action in Eq. (9) does not present particular difficulties; for the Yang-Mills action S_{YM} , we adopt the standard Wilson action [64] (in the following, β will denote the bare coupling $\beta = 6/g^2$), and trace deformations can be rewritten straightforwardly in terms of the lattice variables. The update of the links

directed along spatial directions can be performed by using heat bath and over-relaxation algorithms [65–67] implemented *à la* Cabibbo-Marinari [68], while for the temporal links (which do not enter linearly in the action), we have to resort to a Metropolis update [69].

The procedure we used to assign an integer topological charge value Q to a given configuration is the following [6]: first of all, we reduced the ultraviolet noise present in the configuration by using cooling [70–74] (the numerical equivalence of different smoothing algorithms was shown in several studies; see Refs. [75–80]), and then we computed on the smoothed configurations the quantity $Q_{ni} = \sum_x q_L(x)$, where $q_L(x)$ is the discretization of the topological charge density introduced in Refs. [81,82],

$$q_L(x) = -\frac{1}{2^9 \pi^2} \sum_{\mu\nu\alpha\beta=\pm 1}^{\pm 4} \tilde{\epsilon}_{\mu\nu\alpha\beta} \text{Tr}(\Pi_{\mu\nu}(x)\Pi_{\alpha\beta}(x)). \quad (10)$$

In this expression, $\Pi_{\mu\nu}$ is the plaquette operator, and the modified Levi-Civita tensor $\tilde{\epsilon}_{\mu\nu\alpha\beta}$ coincides with the standard one for positive indices, while its value for negative indices is completely determined by $\tilde{\epsilon}_{\mu\nu\alpha\beta} = -\tilde{\epsilon}_{(-\mu)\nu\alpha\beta}$ and complete antisymmetry. The integer value of the topological charge Q is finally related to Q_{ni} by

$$Q = \text{round}(\alpha Q_{ni}), \quad (11)$$

where “round” stands for the rounding to the closest integer and the constant α was fixed in such a way as to make $\langle (Q - \alpha Q_{ni})^2 \rangle$ as small as possible (see Refs. [6,15] for more details).

From the Monte Carlo history of Q , it is straightforward to estimate the topological susceptibility by using Eq. (5). This is *a priori* possible also for the coefficient b_2 ; however, this is known to not be the most efficient way of extracting it; a b_2 estimator with a more favorable signal-to-noise ratio (especially for large volumes) can be obtained by performing simulations at nonvanishing (imaginary, to avoid the sign problem) values of the topological θ angle [13,15,16].

In practice, if a θ -term of the form $-\theta_L q_L(x)$ is added to the lattice action, b_2 , χ , and the finite lattice renormalization constant of $q_L(x)$ [83] can be extracted from the cumulants of the topological charge distribution at $\theta_L \neq 0$. This approach, although apparently more computationally demanding than the standard one at $\theta_L = 0$, turns out in fact to be much more efficient to obtain reliable estimates of b_2 . For more details, we refer to Ref. [15], where the same method used in the present study was adopted and explained at length.

We finally note that, despite the advantages of the imaginary- θ method, a determination of b_2 is still significantly more challenging than a determination of the topological susceptibility. For this reason, in Sec. III B,

we will use the topological susceptibility when performing a broad scan of the θ -dependence across the phase diagram, while b_2 will be measured only for some specific points.

III. RESULTS

The description of our numerical results is divided in two steps. First, we will discuss the phase structure of the deformed $SU(4)$ gauge theory in the h_1 - h_2 plane and for values of the compactification radius (temperature) for which center symmetry is broken at $h_1 = h_2 = 0$; we will make use of predictions coming from the one-loop effective potential and compare them with results from numerical simulations. In the second part, the θ -dependence which is found in the different phases will be presented and discussed.

A. Phase diagram in the deformation space: One-loop predictions confront numerical results

In the perturbative regime, the effective potential of a translation invariant $SU(4)$ configuration [with $P(\vec{n}) \equiv P$] assumes the form [37]

$$V[P] = \mathcal{E}(P) + h_1 |\text{Tr}P|^2 + h_2 |\text{Tr}P^2|^2, \quad (12)$$

where $\mathcal{E}(P)$ is the one-loop effective potential of the standard Yang-Mills theory computed in Ref. [17]:

$$\mathcal{E}(P) = \sum_{k=1}^{\infty} \frac{1}{k^4} |\text{Tr}P^k|^2. \quad (13)$$

Since Eq. (12) is an $SU(4)$ invariant function, the effective potential can be conveniently rewritten as a function of the three independent eigenvalues of P .

Despite the apparent simplicity of Eq. (12), it is far from trivial to obtain a closed analytical expression for the position of its absolute minimum. It is nevertheless possible to gain some analytical insight into the breaking of center symmetry and the structure of the phase diagram of the $SU(4)$ deformed Yang-Mills theory. Every matrix $M \in SU(4)$ satisfying $\text{Tr}M = \text{Tr}M^2 = 0$ is equivalent to the diagonal matrix with eigenvalues $\lambda_k = e^{i\alpha_k}$ ($k = 0, \dots, 3$), with $\alpha_k = \frac{\pi}{4} + k\frac{\pi}{2}$. If we denote by \mathcal{R} the region of the (h_1, h_2) plane corresponding to points for which $\{\lambda_k\}$ is a local minimum of Eq. (12), the parameter region in which center symmetry is not broken is necessarily a subset of \mathcal{R} , and \mathbb{Z}_4 is surely broken for all the values (h_1, h_2) outside \mathcal{R} . The region \mathcal{R} can be analytically determined, and it can be seen that

$$\mathcal{R} = \left\{ h_1 > \frac{5}{24} \right\} \cap \left\{ h_2 > \frac{1}{96} \right\}, \quad (14)$$

as shown in Fig. 1. In particular, as anticipated, we see that a single deformation is not sufficient to ensure the absence

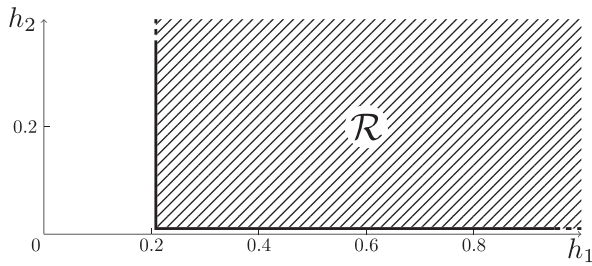


FIG. 1. Graphical representation, in the plane (h_1, h_2) , of the region \mathcal{R} corresponding to points for which $\lambda_k = e^{i\alpha_k}$ ($k = 0, \dots, 3$), with $\alpha_k = \frac{\pi}{4} + k\frac{\pi}{2}$, is a local minimum of the one-loop effective potential.

of center symmetry breaking in the one-loop effective action; the axes $h_1 = 0$ and $h_2 = 0$ lie outside \mathcal{R} , and \mathbb{Z}_4 has to be broken there.

To test the effectiveness of the one-loop potential in predicting the phase diagram, we also numerically investigate the phase diagram of the lattice deformed Yang-Mills theory, using a 6×32^3 lattice and two values of the lattice coupling larger than the critical value $\beta_c \simeq 10.79$ (see Ref. [84]). More in detail, we considered $\beta = 11.15$ (corresponding to an inverse compactification radius $T \simeq 393$ MeV) and $\beta = 11.40$ ($T \simeq 482$ MeV), then performed a scan of the plane (h_1, h_2) in the range $[0, 2] \times [0, 2]$ with a step $\Delta = 0.1$, for a total of 441 simulation points for each β value. The scale has been fixed using the determination of Ref. [84] [see in particular Eq. (35) therein] and fixing the string tension to be $\sigma = (440 \text{ MeV})^2$.

The phase diagram obtained from numerical simulations performed at $\beta = 11.15$ is shown in Fig. 2; in a small region around the origin, \mathbb{Z}_4 is completely broken, while outside, there is no breaking at all, apart from a region at large values of h_1 , where \mathbb{Z}_4 breaks partially to \mathbb{Z}_2 . The different phases have been identified both by looking at histograms of the time histories of $\text{Tr}P$, $\text{Tr}P^2$ (see Figs. 3–5) and by studying³ $\langle |\text{Tr}P| \rangle$, $\langle |\text{Tr}P^2| \rangle$ (see Figs. 6 and 7), where

$$P \equiv \frac{1}{V} \sum_{\vec{n}} P(\vec{n}). \quad (15)$$

The picture that emerges is in striking contrast with the expectations based on the one-loop effective potential: even a single deformation is capable of completely stabilizing center symmetry ($0.2 < h_1 \lesssim 4$ for $h_2 = 0$ or $h_2 > 1.1$ for $h_1 = 0$). This can be noticed by looking at Figs. 5 and 7.

Moving to the larger value of β that we have explored (corresponding to a smaller compactification radius), one may expect that predictions based on the one-loop effective potential get more reliable. The phase diagram obtained for

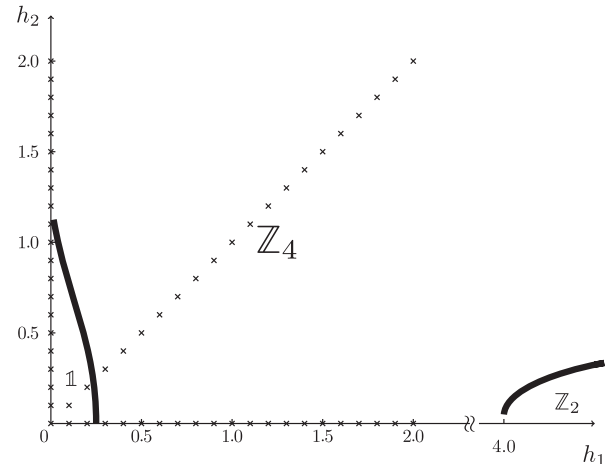


FIG. 2. Phase diagram obtained from simulations performed at bare coupling $\beta = 11.15$ on a 6×32^3 lattice, corresponding to an inverse compactification radius $L^{-1} = T \simeq 393$ MeV. Crosses represent the simulation points where θ -dependence has been explored (see Fig. 11).

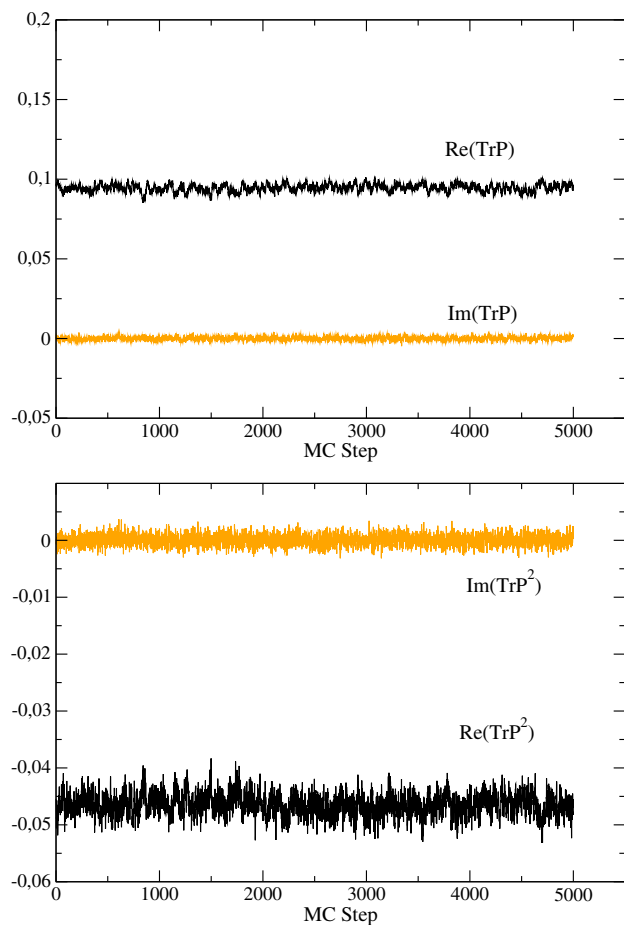


FIG. 3. An example of complete breaking of center symmetry ($\mathbb{Z}_4 \rightarrow \text{Id}$) at $\beta = 11.15$. We report the Monte Carlo histories of $\text{Re}(\text{Tr}P)$, $\text{Im}(\text{Tr}P)$, $\text{Re}(\text{Tr}P^2)$, $\text{Im}(\text{Tr}P^2)$ for $h_1 = 0.0$, $h_2 = 0.1$. Both $\text{Re}(\text{Tr}P)$ and $\text{Re}(\text{Tr}P^2)$ are nonzero.

³Note that $\langle \text{Tr}P \rangle$ and $\langle \text{Tr}P^2 \rangle$ identically vanish on finite lattices, apart from possible numerical issues related to ergodicity breaking for large volumes.

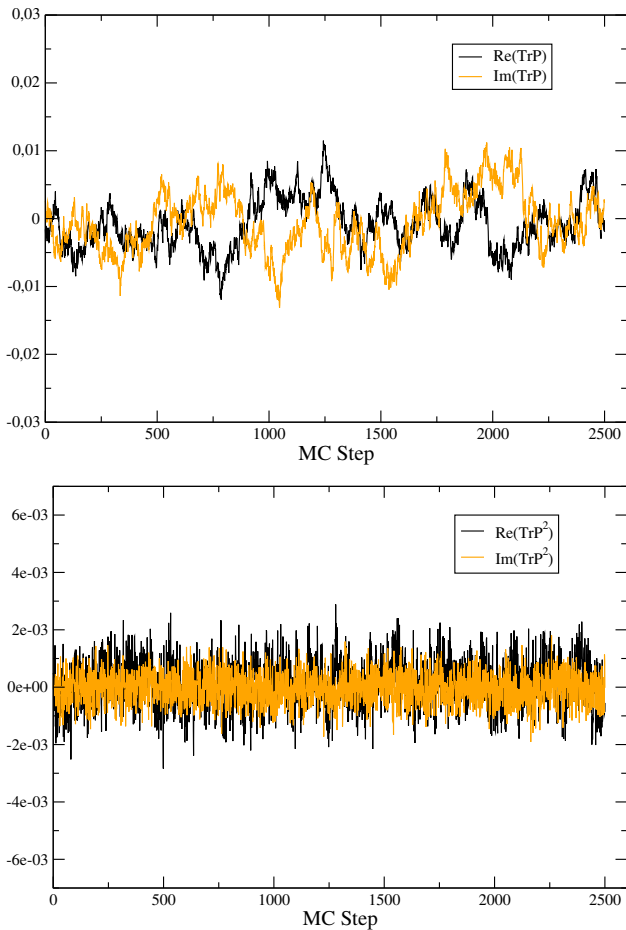


FIG. 4. An example of complete restoration of center symmetry for $\beta = 11.15$, $h_1 = 0.0$, and $h_2 = 1.7$. The Monte Carlo histories of all quantities, $\text{Re}(\text{Tr}P)$, $\text{Im}(\text{Tr}P)$, $\text{Re}(\text{Tr}P^2)$, and $\text{Im}(\text{Tr}P^2)$, fluctuate around their zero average values. It is interesting to notice that the fluctuations of $\text{Tr}P$ are significantly larger than those of $\text{Tr}P^2$; indeed, $\langle P \rangle$ should not be zero according to the one-loop effective potential and vanishes because of long range disorder.

$\beta = 11.40$ is shown in Fig. 8. We can see that indeed the new partially broken phase becomes more manifest, so that center symmetry is now broken along the whole h_1 axis, as predicted in terms of the one-loop potential; however, along the $h_1 = 0$ axis, the discrepancy persists, with center symmetry being protected just by the $|\text{Tr}P^2(\vec{n})|^2$ deformation.

Notice that in sketching Fig. 8 we have not made any statement about the order of the various transition lines. This is an issue that should be considered in future studies, and by now, we can just make some general statements: direct transitions from the completely broken phase to the completely restored phase are expected to be first order, as for the standard deconfining phase transition of $SU(4)$, while transition from the partially restored phase should be in the universality class of the three-dimensional Ising model if they are second order; however, they can still be

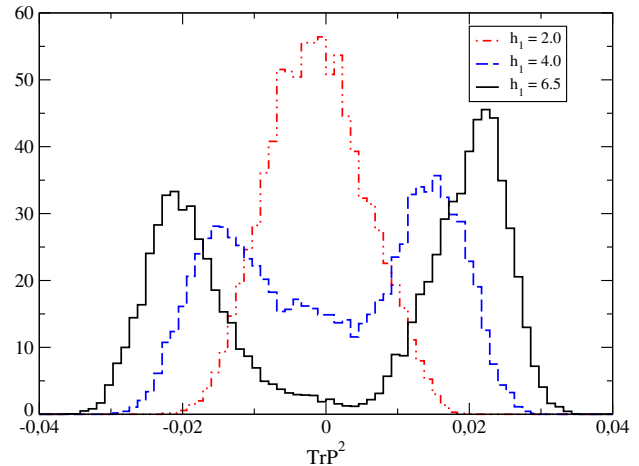


FIG. 5. The histogram of $\text{Re}(\text{Tr}P^2)$ computed using a 6×32^3 lattice at bare coupling $\beta = 11.15$ for three different values of h_1 along the $h_2 = 0$ axis.

first order, and this depends on the dynamics of the system and should be checked by more extensive numerical simulations.

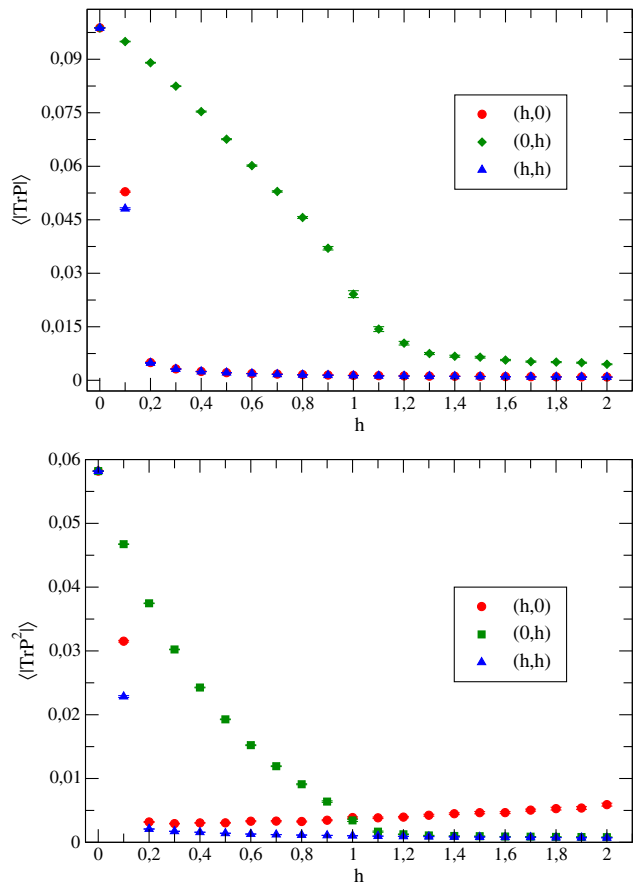


FIG. 6. $\langle |\text{Tr}P| \rangle$ and $\langle |\text{Tr}P^2| \rangle$ computed using a 6×32^3 lattice at bare coupling $\beta = 11.15$ for different values of the deformation parameters. Different datasets correspond to deformations of the form $(h_1 \neq 0, h_2 = 0)$, $(h_1 = 0, h_2 \neq 0)$, and $(h_1 = h_2)$.

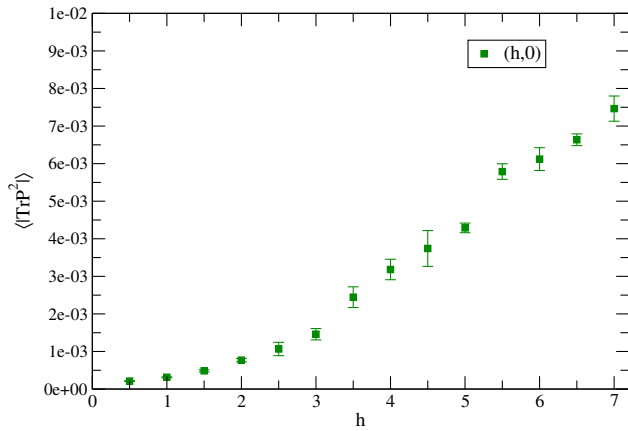


FIG. 7. $\langle |\text{Tr}P^2| \rangle$ computed using a 6×32^3 lattice at bare coupling $\beta = 11.15$ for different values of h_1 along the $h_2 = 0$ axis.

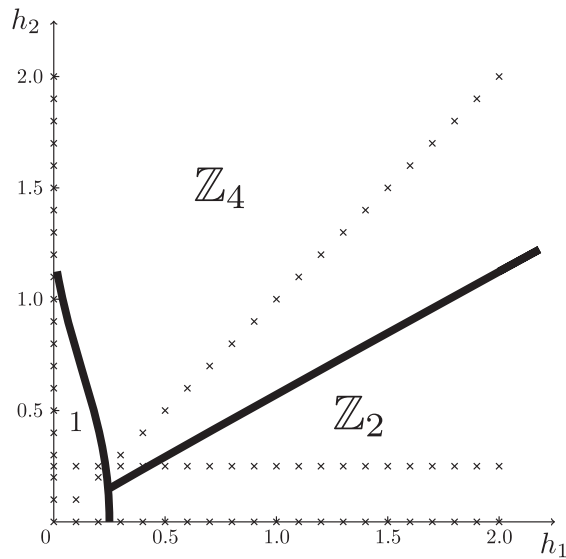


FIG. 8. Phase diagram obtained from simulations performed at bare coupling $\beta = 11.40$ on a 6×32^3 lattice, corresponding to an inverse compactification radius $L^{-1} = T \simeq 482$ MeV. Crosses represent the simulation points where θ -dependence has been explored (see Figs. 13 and 14).

To further investigate the origin of the inconsistencies between the prediction of the one-loop effective potential and the phase diagram observed in numerical simulations, we studied the quantities

$$\langle |\text{Tr}P_{\text{loc}}|^2 \rangle \equiv \frac{1}{\mathcal{V}} \sum_{\vec{n}} \langle |\text{Tr}P(\vec{n})|^2 \rangle \quad (16)$$

$$\langle |\text{Tr}P_{\text{loc}}^2|^2 \rangle \equiv \frac{1}{\mathcal{V}} \sum_{\vec{n}} \langle |\text{Tr}P^2(\vec{n})|^2 \rangle. \quad (17)$$

Since the squared modulus in this case is taken over local, rather than spatially averaged, quantities, such observables

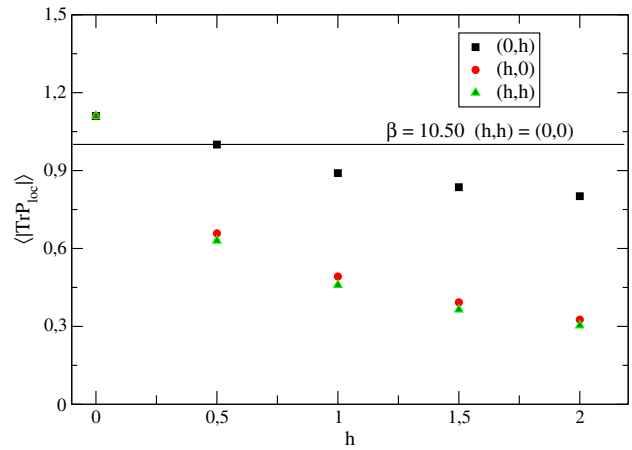


FIG. 9. Mean value of the local quantity $\langle |\text{Tr}P_{\text{loc}}|^2 \rangle$. The black line indicates the value of the undeformed theory for $\beta = 10.50$. The lattice used is 6×32^3 , and the bare coupling $\beta = 11.15$.

should be less sensitive to long range disorder and follow more closely the prediction of the one-loop effective potential.

Our results have been obtained by performing simulations using three different setups for the deformation parameters h_1 and h_2 in Eq. (9). The first two setups are the ones in which only a single deformation is present, i.e., $h_1 \neq 0$ and $h_2 = 0$ or $h_1 = 0$ and $h_2 \neq 0$. The third setup is the one in which both deformations are active and, for the sake of the simplicity, we restricted to the “diagonal” configuration $h_1 = h_2$. We show in particular results obtained for $\beta = 11.15$ on the 6×32^3 lattice (which is one of the two setups already discussed above), which are reported in Figs. 9 and 10 and there compared to reference values obtained on the same lattice and without any deformation at $\beta = 10.50$, which is deep into the confined phase. The corresponding quantities, for which the squared

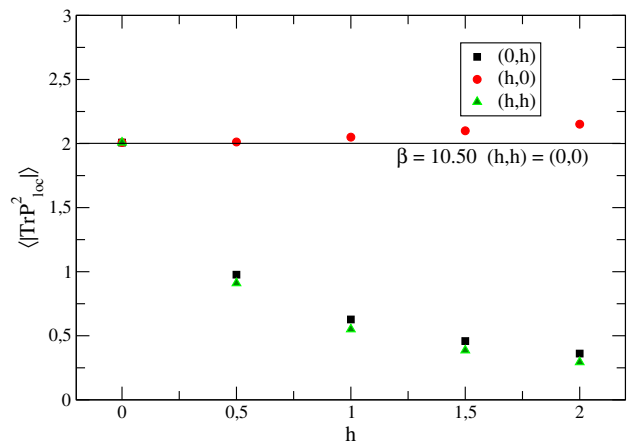


FIG. 10. Mean value of the local quantity $\langle |\text{Tr}P_{\text{loc}}^2|^2 \rangle$. The black line indicates the value of the undeformed theory for $\beta = 10.50$. The lattice used is 6×32^3 , and the bare coupling $\beta = 11.15$.

modulus is taken after the spatial average, have been already shown in Fig. 6.

The general lesson we can learn by comparing the different behaviors is the following. On one hand, it is clear that the local quantities, $\langle |\text{Tr}P_{\text{loc}}|^2 \rangle$ and $\langle |\text{Tr}P_{\text{loc}}^2|^2 \rangle$, are significantly more suppressed, with respect to their values in the standard confined phase, when a direct coupling to the relevant deformation is present (i.e., respectively, $h_1 \neq 0$ or $h_2 \neq 0$); this fact was already noticed and discussed in Ref. [63], pointing to a different kind (from a dynamical point of view) of center symmetry restoration in the trace deformed theory, with respect to the standard confined phase.

On the other hand, when no direct coupling to the relevant deformation is present [i.e., along the $(0, h)$ axis for $\langle |\text{Tr}P_{\text{loc}}| \rangle$ and along the $(h, 0)$ axis for $\langle |\text{Tr}P_{\text{loc}}|^2 \rangle$], the local quantities are not significantly suppressed or remain almost constant, in agreement with the predictions of the one-loop effective potential, meaning that in this case the complete restoration of center symmetry takes place because of long range disorder. This is also appreciable from Fig. 4, where the Monte Carlo histories of the spatially averaged quantities are shown for the same β value and for a point along the $(0, h)$ axis where \mathbb{Z}_4 is completely restored; $\text{Tr}P$, which is not coupled to any deformation, averages to zero, but with much larger fluctuations with respect to $\text{Tr}P^2$, and we interpret this as a manifestation of the fact that $\text{Tr}P$ is locally nonzero but fails to reach an ordered phase at large scales.

B. θ -dependence of the various phases

We are now going to discuss the θ -dependence of the different phases identified previously for the deformed $SU(4)$ theory. It is interesting, in particular, to ask whether the different ways in which \mathbb{Z}_4 can be restored manifest themselves also in a different θ -dependence or not. Let us start from the case of the 6×32^3 lattice at bare coupling $\beta = 11.15$ ($T \approx 393$ MeV), the phase diagram of which was shown in Fig. 2. In Fig. 11, we report the behavior of the topological susceptibility χ as a function of the deformation parameters h_1 and h_2 , for the three deformation setups introduced above. In order to have a direct comparison with the $T = 0$ result, we plot the ratio between the topological susceptibility χ in the deformed theory and the $T = 0$ continuum value computed in ordinary Yang-Mills theory in Ref. [16]. We are using here the fact, explicitly verified in Ref. [63], that the lattice spacing can be considered to be independent of the deformation for all practical purposes. This will not be necessary in the following when discussing results for b_2 , since b_2 is dimensionless.

For $h_1 = h_2 = 0$, the system at $\beta = 11.15$ is in the deconfined phase, so we expect the value of the topological susceptibility χ to be tiny for small values of the deformation parameters. From data in Fig. 11, we see that this is

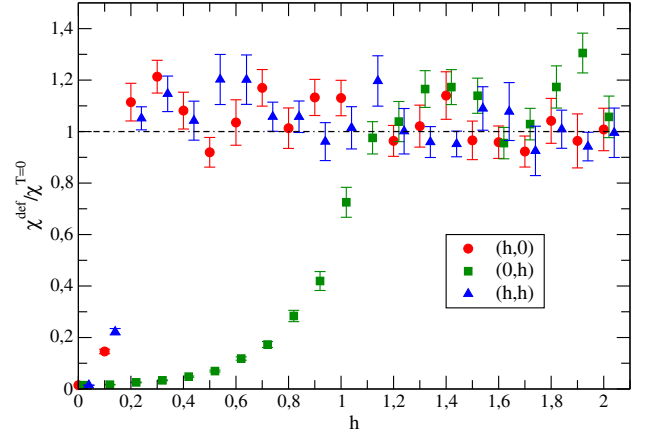


FIG. 11. Ratio between the topological susceptibility χ computed in the deformed theory and the one at $T = 0$ computed in Ref. [16] for different values of the deformation parameters h_1 and h_2 . Results are obtained on the 6×32^3 lattice at bare coupling $\beta = 11.15$.

indeed the case for all the deformation setups studied. Moreover, the topological susceptibility always reaches a plateau for large deformations, at a value which is consistent with that of χ measured at $T = 0$ in ordinary Yang-Mills theory. This asymptotic value is, however, approached differently in the different deformation setups: when using $h_2 = 0$ or $h_1 = h_2$, the plateau starts from $h \approx 0.2$, while in the setup with $h_1 = 0$, it starts from $h \approx 1.2$. The reason for this behavior is clear from the phase diagram shown in Fig. 2: these values of the deformation parameters are the ones that are needed to reach the \mathbb{Z}_4 -symmetric phase when moving along the axes or along the diagonal of the phase diagram.

Using the same lattice setting, we computed also the coefficient b_2 related to the fourth power of θ in the expansion of the free energy; see Eq. (4). As explained in Sec. II, the estimation of b_2 is computationally much more demanding than that of χ ; for this reason, we decided to compute b_2 just for three values of the deformations deep in the plateau region, one for each of the three deformation setups previously adopted (with $h = 1.5$ in all the cases). We computed b_2 by means of the imaginary θ method discussed in Sec. II, using seven values of θ_L in the range $[0, 12]$. The outcome of this analysis is reported in Fig. 12: also for b_2 , there is a nice agreement between the values computed in the deformed theory in the \mathbb{Z}_4 restored phase and the one obtained in the $T = 0$ Yang-Mills case, for all the deformation setups.

It is interesting to compare the results obtained for b_2 with the values predicted by using two well-known approximation schemes. The first one is the DIGA, which is expected to be reliable in ordinary Yang-Mills theory for a small value of the compactification radius. In this approximation, the system is supposed to be well approximated by a gas of weakly interacting degrees of freedom

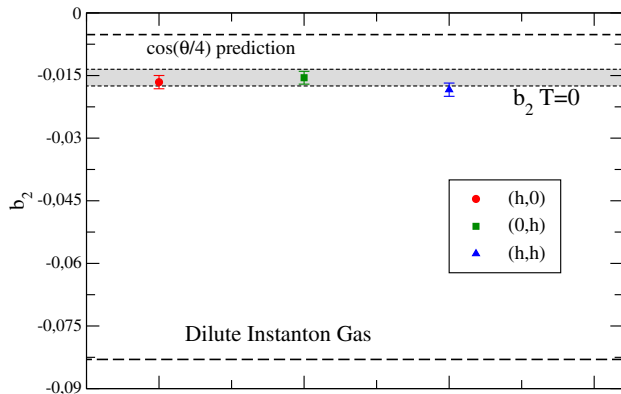


FIG. 12. The coefficient b_2 measured in the deformed theory on the 6×32^3 lattice at $\beta = 11.15$, for the different deformation setups and $h = 1.5$. The band denotes the $T = 0$ continuum result computed in Ref. [16], while the dashed lines indicate the DIGA ($-1/12$) and the DFIGA predictions ($-1/192$).

(d.o.f.), carrying an unit of topological charge (± 1), and the coefficient b_2 is predicted to be $-1/12$. The second approximation scheme is the DFIGA, which is expected to be valid in the center-symmetric phase of the deformed theory for small values of the compactification length. In this case, the d.o.f. are still expected to be weakly interacting, but now they carry a fractional topological charge, quantized in units of $1/N$. In this scenario, the predicted value is $b_2 = -1/(12N^2)$, i.e., $b_2 = -1/192$ for $SU(4)$. Both these values are shown in Fig. 12, and they are clearly not compatible with numerical data, indicating that the compactification length used is still too large for the interactions between the fractional d.o.f. to be negligible.

Let us now repeat the same analysis for the second value of the bare coupling constant β studied in Sec. III A, i.e., $\beta = 11.40$ (corresponding to $T \approx 482$ MeV). The values of the deformations used are $0 \leq h_1 \leq 2$ and $0 \leq h_2 \leq 2$. Three different phases are present, see Fig. 8, and one could expect that also the θ -dependence shows some signal of the presence of the phase with \mathbb{Z}_4 broken to \mathbb{Z}_2 .

From Fig. 13, where the results for the topological susceptibility are reported, we see that this is indeed the case; errors are larger than for $\beta = 11.15$, but it is quite clear that the values of χ approach $\chi_{T=0}$ only for two of the three deformation setups adopted, namely the one in which $h_1 = 0$ and the one in which $h_1 = h_2$. By looking at the phase diagram in Fig. 8, we see that these are the only two setups in which the deformations induce a complete restoration of the center symmetry and that the values of the deformation at which the plateaux are reached are consistent with the boundaries of the region with broken center symmetry. In the remaining deformation setup, in which $h_2 = 0$, center symmetry is not completely restored by increasing the value of h_1 , and the system enters the phase in which center symmetry is broken to its \mathbb{Z}_2 subgroup. While it is not clear why in this phase the

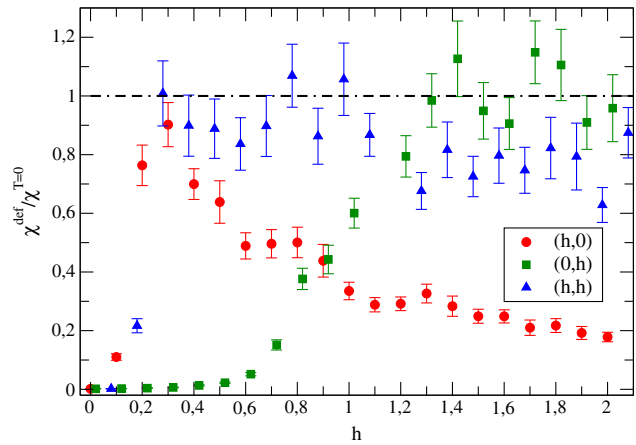


FIG. 13. Ratio between the topological susceptibility χ computed in the deformed theory and at the one at $T = 0$ continuum from Ref. [16] for different values of the deformation parameters h_1 and h_2 . Results are obtained on the lattice 6×32^3 at bare coupling $\beta = 11.40$.

susceptibility seems to approach zero as we increase h_1 , it is tempting to interpret the peak at $h \approx 0.3$ (at which point $\chi \approx \chi_T$) as a proximity effect due to the closeness of the completely restored phase in the phase diagram (see Fig. 8). In order to investigate this hypothesis, we computed the value of the topological susceptibility also using a different setup, i.e., varying h_1 and keeping $h_2 = 0.25$, because from the phase diagram of Fig. 8, we see that in this setup the system passes across all the symmetry breaking patterns. Results are shown in Fig. 14. We can clearly see that the case $(h_1, h_2 = 0.25)$ is in between the diagonal case and the one with only the h_1 deformation; the values of the deformation parameter at which the topological

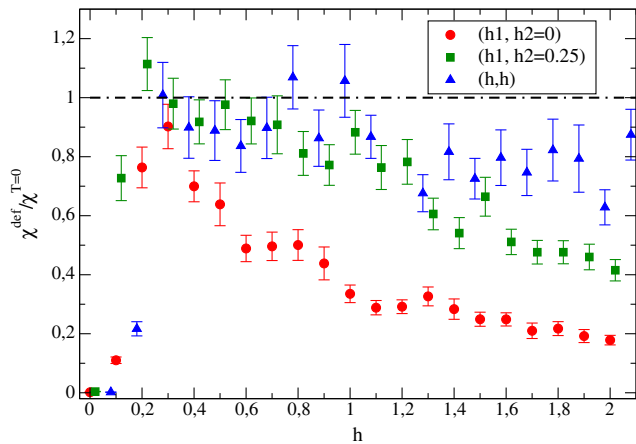


FIG. 14. Ratio between the topological susceptibility χ computed in the deformed theory and at the one at the $T = 0$ continuum from Ref. [16] for different values of the deformation parameters h_1 and h_2 . In particular, here we report the case in which h_1 varies and h_2 is kept fixed at $h_2 = 0.25$. Results are obtained on the 6×32^3 lattice at bare coupling $\beta = 11.40$.

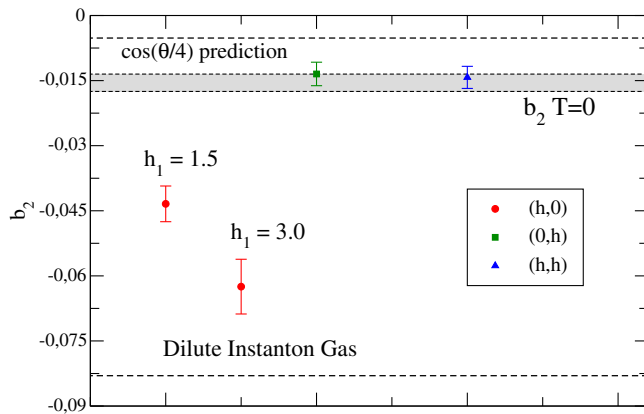


FIG. 15. The coefficient b_2 measured in the deformed theory on the 6×32^3 lattice at $\beta = 11.40$, for the different deformation setups and $h = 1.5$ (apart from the point indicated by $h_1 = 3.0$). The band denotes the $T = 0$ continuum result of Ref. [16], while the dashed lines indicate the DIGA ($-1/12$) and the DFIGA predictions ($-1/192$).

susceptibility is compatible with the one at $T = 0$ correspond to the region in which center symmetry is completely restored, and this can be appreciated when comparing with the phase diagram shown in Fig. 8.

The presence of the partially broken phase is evident also from the values of b_2 computed at $\beta = 11.40$, which are shown in Fig. 15. The values of b_2 in the phase with completely restored center symmetry are again compatible with the results obtained at $T = 0$ in Ref. [16], while the values corresponding to the deformation parameters $h_1 = 1.5$, $h_2 = 0$ and $h_1 = 3.0$, $h_2 = 0$ are incompatible with $b_2(T = 0)$ and lie in the middle between the DIGA prediction $-1/12$ and the DFIGA one $-1/192$.

Altogether, lattice data indicate that the θ -dependence of the deformed theory coincides with the one of ordinary Yang-Mills theory at $T = 0$ only when center symmetry is completely recovered, and this happens independently of the specific way the restoration takes place, i.e., either by local suppression of $\text{Tr}P$ and $\text{Tr}P^2$ or by long range disorder. Instead, in the phase in which center symmetry is only partially restored, neither the topological susceptibility nor b_2 reaches a clear plateau as a function of the deformation parameter, and they assume values somewhere in between the deconfined and the confined cases.

IV. CONCLUSIONS

In this paper, we have investigated the relation between center symmetry and θ -dependence in Yang-Mills theories, exploiting trace deformations in order to control the realization of center symmetry breaking in a theory with a small compactified direction. Extending previous results presented in Ref. [63] for the $SU(3)$ pure gauge theory, we have considered $SU(4)$, which is particularly interesting since, apart from allowing a larger space of independent

trace deformations, it is also the first $SU(N)$ gauge group for which the center group admits various patterns of symmetry breaking.

In a first step, we have investigated the phase diagram of the theory in the deformation space and for various values of the inverse compactified radius, reaching values up to $L^{-1} \sim 500$ MeV. We have considered predictions from the one-loop effective potential of the Polyakov loop and compared them to results of numerical lattice simulations, in which the fate of center symmetry breaking has been studied both by global (i.e., averaged over all directions orthogonal to the compactified direction) and local quantities. We have shown that center symmetry in the deformed theory can be completely restored in a way which is sometimes qualitatively different from that of the standard confined phase, as evinced from the expectation value of local quantities directly coupled to the deformations, and sometimes in contrast with expectations from the one-loop effective potential, since the restoration takes place through long range disorder.

Despite this variety of possible restorations, our numerical results show that the θ -dependence of the deformed theory matches, within statistical errors, that of the standard confined phase in all cases in which center symmetry is completely restored. On the contrary, a partial restoration of center symmetry leads to a θ -dependence which is different from both that of the confined phase and that of the deconfined phase, interpolating in some way between them.

The failure to reproduce predictions for the θ -dependence coming from semiclassical computations (in particular those equivalent to a sort of DFIGA) can be ascribed, as for the $SU(3)$ results reported in Ref. [63], to the fact that our inverse compactifications radius is still not large. On the other hand, the striking agreement with results from the standard confined phase confirms and reinforces the evidence, already shown for $SU(3)$, for a strict relation between the fate of center symmetry and other relevant nonperturbative features of Yang-Mills theories. This can be viewed as a practical realization of the volume independence which is expected to hold in the large- N limit as soon as no phase transition is crossed.

Future studies could extend the present investigation in various directions. Considering other relevant nonperturbative properties, such as the spectrum of glueball masses, is a first nontrivial goal that should be pursued. The extension to large $SU(N)$ gauge groups is of course another interesting direction.

ACKNOWLEDGMENTS

Numerical simulations have been performed at the Scientific Computing Center at INFN-PISA and on the MARCONI machine at CINECA, based on IS CRA Project No. IsB18-TD DYM.

- [1] E. Vicari and H. Panagopoulos, *Phys. Rep.* **470**, 93 (2009).
- [2] G. 't Hooft, *Nucl. Phys.* **B72**, 461 (1974).
- [3] E. Witten, *Ann. Phys. (N.Y.)* **128**, 363 (1980).
- [4] E. Witten, *Phys. Rev. Lett.* **81**, 2862 (1998).
- [5] B. Lucini and M. Teper, *J. High Energy Phys.* **06** (2001) 050.
- [6] L. Del Debbio, H. Panagopoulos, and E. Vicari, *J. High Energy Phys.* **08** (2002) 044.
- [7] B. Lucini, M. Teper, and U. Wenger, *Nucl. Phys.* **B715**, 461 (2005).
- [8] M. Cè, M. G. Vera, L. Giusti, and S. Schaefer, *Phys. Lett. B* **762**, 232 (2016).
- [9] E. Witten, *Nucl. Phys.* **B156**, 269 (1979).
- [10] G. Veneziano, *Nucl. Phys.* **B159**, 213 (1979).
- [11] M. D'Elia, *Nucl. Phys.* **B661**, 139 (2003).
- [12] L. Giusti, S. Petrarca, and B. Taglienti, *Phys. Rev. D* **76**, 094510 (2007).
- [13] H. Panagopoulos and E. Vicari, *J. High Energy Phys.* **11** (2011) 119.
- [14] M. Cè, C. Consonni, G. P. Engel, and L. Giusti, *Phys. Rev. D* **92**, 074502 (2015).
- [15] C. Bonati, M. D'Elia, and A. Scapellato, *Phys. Rev. D* **93**, 025028 (2016).
- [16] C. Bonati, M. D'Elia, P. Rossi, and E. Vicari, *Phys. Rev. D* **94**, 085017 (2016).
- [17] D. J. Gross, R. D. Pisarski, and L. G. Yaffe, *Rev. Mod. Phys.* **53**, 43 (1981).
- [18] C. G. Callan, R. Dashen, and D. J. Gross, *Phys. Rev. D* **17**, 2717 (1978).
- [19] D. Kharzeev, R. D. Pisarski, and M. H. G. Tytgat, *Phys. Rev. Lett.* **81**, 512 (1998).
- [20] O. Bergman and G. Lifschytz, *J. High Energy Phys.* **04** (2007) 043.
- [21] A. Parnachev and A. R. Zhitnitsky, *Phys. Rev. D* **78**, 125002 (2008).
- [22] B. Allés, M. D'Elia, and A. Di Giacomo, *Nucl. Phys.* **B494**, 281 (1997); **B679**, 397(E) (2004); *Phys. Lett. B* **412**, 119 (1997); **483**, 139 (2000).
- [23] C. Gattringer, R. Hoffmann, and S. Schaefer, *Phys. Lett. B* **535**, 358 (2002).
- [24] L. Del Debbio, H. Panagopoulos, and E. Vicari, *J. High Energy Phys.* **09** (2004) 028.
- [25] E. Berkowitz, M. I. Buchoff, and E. Rinaldi, *Phys. Rev. D* **92**, 034507 (2015).
- [26] S. Borsanyi, M. Dierigl, Z. Fodor, S. D. Katz, S. W. Mages, D. Nogradi, J. Redondo, A. Ringwald, and K. K. Szabo, *Phys. Lett. B* **752**, 175 (2016).
- [27] P. Rossi, *Phys. Rev. D* **94**, 045013 (2016).
- [28] C. Bonanno, C. Bonati, and M. D'Elia, *J. High Energy Phys.* **01** (2019) 003.
- [29] M. Berni, C. Bonanno, and M. D'Elia, *Phys. Rev. D* **100**, 114509 (2019).
- [30] P. Di Vecchia and G. Veneziano, *Nucl. Phys.* **B171**, 253 (1980).
- [31] G. G. di Cortona, E. Hardy, J. P. Vega, and G. Villadoro, *J. High Energy Phys.* **01** (2016) 034.
- [32] C. Bonati, M. D'Elia, M. Mariti, G. Martinelli, M. Mesiti, F. Negro, F. Sanfilippo, and G. Villadoro, *J. High Energy Phys.* **03** (2016) 155.
- [33] C. Bonati, M. D'Elia, H. Panagopoulos, and E. Vicari, *Phys. Rev. Lett.* **110**, 252003 (2013).
- [34] E. Poppitz, T. Schaefer, and M. Unsal, *J. High Energy Phys.* **03** (2013) 087.
- [35] M. D'Elia and F. Negro, *Phys. Rev. Lett.* **109**, 072001 (2012).
- [36] M. D'Elia and F. Negro, *Phys. Rev. D* **88**, 034503 (2013).
- [37] M. Unsal and L. G. Yaffe, *Phys. Rev. D* **78**, 065035 (2008).
- [38] J. C. Myers and M. C. Ogilvie, *Phys. Rev. D* **77**, 125030 (2008).
- [39] P. Kovtun, M. Unsal, and L. G. Yaffe, *J. High Energy Phys.* **06** (2007) 019.
- [40] M. Unsal, *Phys. Rev. Lett.* **100**, 032005 (2008).
- [41] M. Unsal, *Phys. Rev. D* **80**, 065001 (2009).
- [42] M. Shifman and M. Unsal, *Phys. Rev. D* **78**, 065004 (2008).
- [43] J. C. Myers and M. C. Ogilvie, *J. High Energy Phys.* **07** (2009) 095.
- [44] G. Cossu and M. D'Elia, *J. High Energy Phys.* **07** (2009) 048.
- [45] P. N. Meisinger and M. C. Ogilvie, *Phys. Rev. D* **81**, 025012 (2010).
- [46] M. Unsal and L. G. Yaffe, *J. High Energy Phys.* **08** (2010) 030.
- [47] E. Thomas and A. R. Zhitnitsky, *Phys. Rev. D* **86**, 065029 (2012).
- [48] E. Poppitz, T. Schaefer, and M. Unsal, *J. High Energy Phys.* **10** (2012) 115.
- [49] E. Thomas and A. R. Zhitnitsky, *Phys. Rev. D* **87**, 085027 (2013).
- [50] E. Poppitz, T. Schaefer, and M. Unsal, *J. High Energy Phys.* **03** (2013) 087.
- [51] T. Misumi and T. Kanazawa, *J. High Energy Phys.* **06** (2014) 181.
- [52] M. M. Anber, E. Poppitz, and B. Teeple, *J. High Energy Phys.* **09** (2014) 040.
- [53] A. Bhoonah, E. Thomas, and A. R. Zhitnitsky, *Nucl. Phys.* **B890**, 30 (2014).
- [54] A. Cherman, S. Sen, M. L. Wagman, and L. G. Yaffe, *Phys. Rev. D* **95**, 074512 (2017).
- [55] T. Sulejmanpasic, *Phys. Rev. Lett.* **118**, 011601 (2017).
- [56] M. M. Anber and A. R. Zhitnitsky, *Phys. Rev. D* **96**, 074022 (2017).
- [57] Y. Tanizaki and M. Unsal, [arXiv:1912.01033](https://arxiv.org/abs/1912.01033).
- [58] E. Itou, *J. High Energy Phys.* **05** (2019) 093.
- [59] G. Bergner, S. Piemonte, and M. Ünsal, *J. High Energy Phys.* **11** (2018) 092.
- [60] E. Thomas and A. R. Zhitnitsky, *Phys. Rev. D* **85**, 044039 (2012).
- [61] M. Unsal, *Phys. Rev. D* **86**, 105012 (2012).
- [62] K. Aitken, A. Cherman, and M. Ünsal, *J. High Energy Phys.* **09** (2018) 030.
- [63] C. Bonati, M. Cardinali, and M. D'Elia, *Phys. Rev. D* **98**, 054508 (2018).
- [64] K. G. Wilson, *Phys. Rev. D* **10**, 2445 (1974).
- [65] M. Creutz, *Phys. Rev. D* **21**, 2308 (1980).
- [66] A. D. Kennedy and B. J. Pendleton, *Phys. Lett.* **156B**, 393 (1985).
- [67] M. Creutz, *Phys. Rev. D* **36**, 515 (1987).
- [68] N. Cabibbo and E. Marinari, *Phys. Lett.* **119B**, 387 (1982).

- [69] N. Metropolis, A. W. Rosenbluth, M. N. Rosenbluth, A. H. Teller, and E. Teller, *J. Chem. Phys.* **21**, 1087 (1953).
- [70] B. Berg, *Phys. Lett.* **104B**, 475 (1981).
- [71] Y. Iwasaki and T. Yoshie, *Phys. Lett.* **131B**, 159 (1983).
- [72] S. Itoh, Y. Iwasaki, and T. Yoshie, *Phys. Lett.* **147B**, 141 (1984).
- [73] M. Teper, *Phys. Lett.* **162B**, 357 (1985).
- [74] E. M. Ilgenfritz, M. L. Laursen, G. Schierholz, M. Muller-Preussker, and H. Schiller, *Nucl. Phys.* **B268**, 693 (1986).
- [75] C. Bonati and M. D'Elia, *Phys. Rev. D* **89**, 105005 (2014).
- [76] K. Cichy, A. Dromard, E. Garcia-Ramos, K. Ottnad, C. Urbach, M. Wagner, U. Wenger, and F. Zimmermann, *Proc. Sci., LATTICE2014* (**2014**) 075 [[arXiv:1411.1205](https://arxiv.org/abs/1411.1205)].
- [77] Y. Namekawa, *Proc. Sci., LATTICE2014* (**2015**) 344.
- [78] C. Alexandrou, A. Athenodorou, and K. Jansen, *Phys. Rev. D* **92**, 125014 (2015).
- [79] C. Alexandrou, A. Athenodorou, K. Cichy, A. Dromard, E. Garcia-Ramos, K. Jansen, U. Wenger, and F. Zimmermann, [arXiv:1708.00696](https://arxiv.org/abs/1708.00696).
- [80] B. A. Berg and D. A. Clarke, *Phys. Rev. D* **95**, 094508 (2017).
- [81] P. Di Vecchia, K. Fabricius, G. C. Rossi, and G. Veneziano, *Nucl. Phys.* **B192**, 392 (1981).
- [82] P. Di Vecchia, K. Fabricius, G. C. Rossi, and G. Veneziano, *Phys. Lett.* **108B**, 323 (1982).
- [83] M. Campostrini, A. Di Giacomo, and H. Panagopoulos, *Phys. Lett. B* **212**, 206 (1988).
- [84] B. Lucini, M. Teper, and U. Wenger, *J. High Energy Phys.* **02** (2005) 033.